SILMARIL: Optical Layout and Implementation.

CHARA Technical Report #105

Theo ten Brummelaar, Peter Tuthill & Cyprien Lanthermann

Version 11: 2021-12-16

1.0 INTRODUCTION

This document is a description of the design of the SILMARIL (CC++) combiner. More detailed modeling and ray tracing have been performed and will be written up in a separate document, but we wanted to first be satisfied that the design is feasible.

The primary aim of this beam combiner is to maximize sensitivity. It needs to combine at least three beams and, if possible, more. Some spectral resolution is also required for group delay tracking. We have settled on an image plane beam combiner. See TR103 for a discussion of this design choice.

This design is based on Peter's "Iron Throne" concept (Figure 1.) that uses very long focal length cylindrical (CL1) mirrors to form the image in the fringe axis (horizontal), and a much shorter focal length second cylindrical lens (CL2) to form the image in the spectrograph axis (vertical). The intent, based on the desire to optimize for faint light operation, is to minimize the number of optics and reduce background in K´ band as much as possible, while at the same time allowing a development path that enables us to test the fundamental optical design on the sky without using a second dewar. For ultimate performance an upgrade including a second dewar with specialized cold stops is planned and funded.

In summary, we are confident that the design presented here will work and is optimized for faint targets as required. More complete ray tracing is underway to determine the complete specifications and tolerances of the optical components. We know enough now to order the detector, and this has been done. There is a 12-month lead time for the camera, but the options of changing the internal filters and the shape of the cold stop inside the camera dewar are open during most of that time. Work will continue in building the optical system in the laboratory in the meantime using the engineering grade camera already purchased.

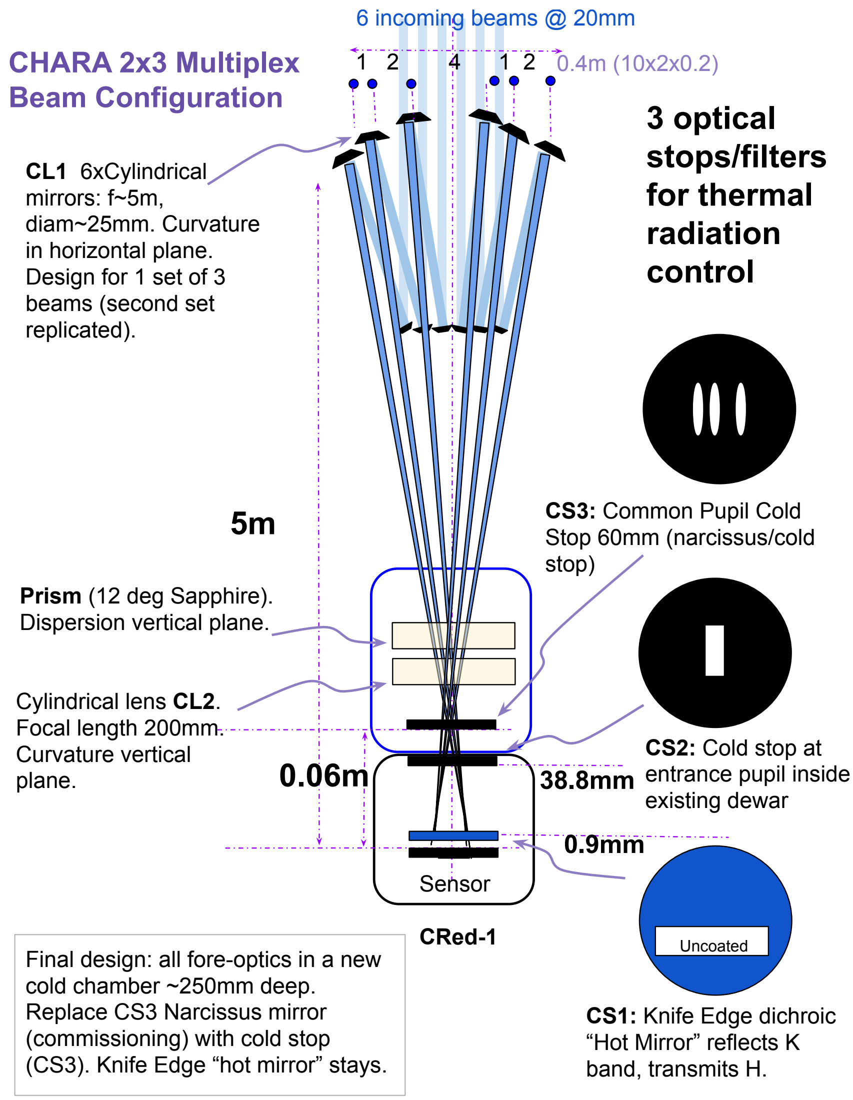

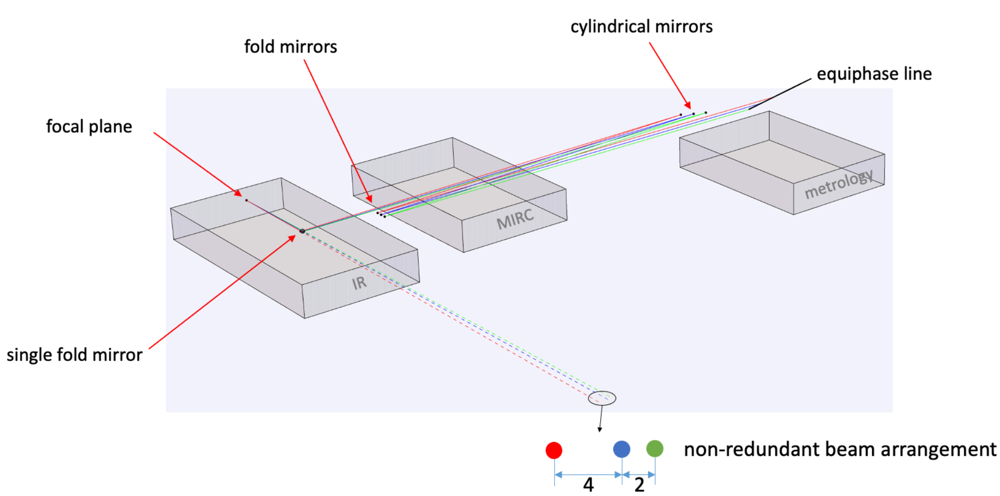

Figure 1. Basic layout of Peter's "Iron Throne" concept. Note that the dimensions in this diagram are nominal and based on estimates made at the time it was drawn.

2.0 OPTICAL LAYOUT

For the first part of this report, we consider only a single 3-beam combiner: the minimum required number of beams. A 4-beam device uses more than twice as many pixels, and therefore violates the design brief to aim for 3-beam sensitivity above all other considerations. Multiplexing of 2 independent sets of 3 is dealt with later in this report. It will be shown that this facility can be added with no compromise at all to the performance of the single set of 3.

Mirrors at the standard beam height are used to send the beams to long focal length cylindrical mirrors CL1 at a higher level. These cylindrical mirrors are arrayed in the standard 2-4-6 non-redundant beam pattern and send the beams to a common focal point in the horizontal axis. These are followed by a second cylindrical lens CL2 acting in the vertical axis and of shorter focal length. This compresses the image to a small number of pixels in the vertical axis. When used in concert with a vertical dispersive element, the instrument now yields a modest spectral resolution, a layout usually termed *channel spectrum fringes*. An extra fold mirror - or possibly CL2 serving a dual role - as shown at the bottom of Figure 1, may be necessary to fit things into the available space.

This arrangement has minimal optics and will produce an image that can be placed directly onto the CRED-1 camera. At a later time, we intend to add a fore-dewar based largely on the MYSTIC design.

We will now consider each of the optical elements in turn.

2.1 Folding Mirrors

These need not be anything fancy. A standard λ/20 mirror with tiptilt mount, for example a Zaber mount, and a kinematic base should be fine. Rather than stagger the cylindrical mirrors to achieve the correct relative phase of the beams, as shown in Figure 1, we should stagger these fold mirrors if space allows. This way we can use the STS for alignment and phasing.

2.2 Cylindrical Mirror #CL1

The design begins with the native CHARA lab beam diameter. Here this is assumed D=19mm and in the light of maximizing sensitivity, we consider only one triplet. Expansion to two triplets is given in Section 6. Our triplet needs to be formatted into a pupil occupying a space 1D by 7D (Figure 2).

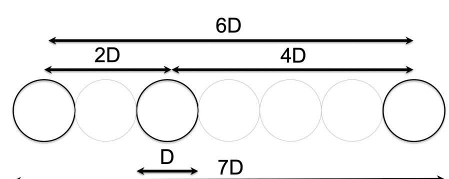

Figure 2. Beam layout for three beam combination.

Strict Nyquist sampling wastes Fourier power (50% at the limit); a common rule of thumb is to sample at least 1.5× more densely so 3 pixels per fringe, however this requires more pixels. A compromise is to follow the design of MYSTIC and use 2.5 pixels per fringe, which we will assume here. For a maximum separation of nD, there will be $2.44n$ fringes across the image. For $n = 7$ this is 17 fringes and requires 43 pixels for the shortest wavelength channel and 67 for the longest. The focal length of these mirrors is very long and is not a driving factor in the rest of the design.

Sourcing manufacture of CL1 is a risk custom element of the design. Very long focal length cylindrical mirrors are not available off the shelf, but options do exist. To get a feel for the specifications of CL1 we start with the required wavelength regime for the device. We will assume that this will be both the H and K´ bands currently available in NIRO as set out in Table 1. Note that the cutoff wavelengths have been adjusted slightly to match those standard in Astronomy for these bands.

Table 1. NIRO Filters in microns.

Band	Center	Width	Short End	Long End
H	1.635	0.29	1.49	1.78
K′	2.150	0.32	1.99	2.31

With 17 fringes across the size of the Airy disk across 43 pixels that are 24 μm across at the shortest wavelength of λ = 1.49 μm the focal length of CL1 will be

$$F = \frac{43 \times 24\, D}{2.44\, \lambda} = 5.408 \text{ m}$$

The tolerance on the focal length is forgiving for the absolute length but more difficult for the difference in focal length between the optics. We need the images from the three beams to remain within the far-field of the optical system so that the pattern will scale with errors in focal length rather than change shape. To be in the far-field the Fresnel number must be less than 1

$$F = \frac{R^2}{\lambda O} \ll 1.0$$

where O is the object distance. For a perfect lens $O = \infty$ so $F = 0$, as one would expect. If the image is a distance z instead of the focal length f the simple lens equation tells us that

$$O = \frac{fz}{z - f}$$

so the image position to yield a given Fresnel number F is

$$z = \frac{R^2 f}{R^2 - F\,\lambda\, f}$$

which is plotted in Figure 3 for the focal length of 5.4 m, beam radius of 0.019 m and the shortest wavelength of the H band channel. A Fresnel number of less than 0.1 means that the focal length of the cylindrical optics must match to within 0.25%. At 1% the Fresnel number is about. 0.5. A focal length error of less than 1% is not an unusual constraint on optics.

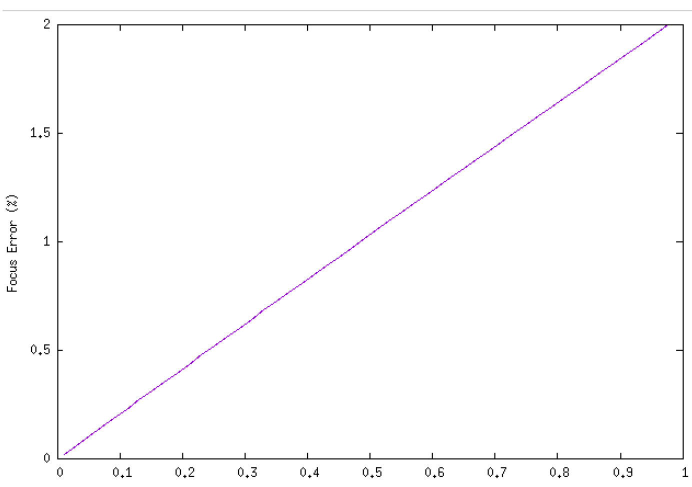

Figure 3. Focal error Vs Fresnel number for a 2cm beam, focal length of 5.463m and the short end of H band.

Cylindrical lenses with such large focal lengths will be a custom optic of some kind. The possibilities we know of so far are:

1. An optic made using a diamond lathe. Mike Ireland has said it should be possible to manufacture something at ANU. We also had a brief exchange with the company CMM Optics who said that making a one wave peak-to-peak optic would be about \$2.5k per device, A 20th wave peak-to-peak optic is possible but would cost \$9k each with a setup cost of \$20k, so \$16k each. A more recent estimate was for \$5.5k for a 20th wave optic. One drawback of a tool optic like this is that

there will be large scattering and other affects in the optical which may make initial alignment using visible light more difficult.

2. The long radius of curvature means that the maximum deviation of the surface is less than 5μm so we could use a deformable mirror. This has the added attraction that we may be able to correct for other optical issues, but it will be expensive. The OKO PDM30 has 19 channels, is 30mm in diameter, and has a cost of about $14.5k, so not very different from the 20th wave optic above. ALPAO have similar devices and have modeled putting a cylindrical surface on one of their DMs resulting in a 40nm rms error. The disadvantage of using a DM here is that they suffer from hysteresis, are not good at holding a static shape, and may require a wavefront sensor or some other sort of image quality metric.
3. We could use a cylindrical lens instead of a mirror. This would add a reflection to the system and would have the same tolerances as the mirror.
4. Other solutions include bending a flat optic with some pressure on either side, or a two-lens arrangement, with opposed positive and negative lenses.

It is the cost and availability of obtaining this long focal length cylindrical element that will dominate the practicality of this design, and we will assume option 1 as a baseline in the design.

2.3 Cylindrical Lens/Mirror #CL2

This needs to concentrate light in the vertical direction as much as possible, ideally into a single pixel. Assuming the beam diameter is 19mm and the longest wavelength 2.31 microns, then the full angle of the diffraction Airy disk is $2.44 \times 2.31\ \mu m / 0.019 m = 2.97\times10^{-4}$ radians. For this to fill one 24 μm pixel, the focal distance is 81mm. As we shall see below, this is much faster than the First Light default cold stop F ratio of 20, and it is this that will drive the focal length of CL2.

This highlights a central design tradeoff in specifying this instrument. For best spectral performance, a short-focal length of 81mm is indicated, although actual resolution R only degrades somewhat slowly with longer focal lengths. For example, only a factor less than 2 in K′ when doubling CL2 to 164mm. However, short focal lengths result in a larger beam in the vertical direction at the cold stop. So, the area of outside world visible to the camera, hence the thermal load, scales linearly (not as the square) with the inverse of this length. The compromise to be struck is this: better thermal performance from a longer vertical-direction f-ratio must be traded against better spectral sampling from a short focus CL2. Note that the horizontal f-ratio is fixed by fringe sampling and does not enter this debate.

It seems that the likely boundaries for this trade-off lie between about 200mm which has moderately good spectral sampling but a larger cold stop giving a total f-ratio equivalent of about f-10, to about 400mm which matches the F-20 of the default First Light system but notably degraded spectral performance. We have settled on a compromise focal length of 350mm as this gives a similar vertical size for the cold stop as the horizontal size determined by the fringe spacing. This lens should be no more difficult to acquire than CL1.

2.4 Dispersive Element

The amount of dispersion is a compromise between the number of pixels we read out and the length of delay space covered for group delay tracking. More spectral resolution could also be used, but this entangles several design trades and choices.

The resolution obtained by the spectrometer depends on two things: the strength of the dispersing element *and* the point-spread function in the dispersion direction, so the values discussed above in the choice of CL2 will impact the spectral performance. It is important to keep in mind the design brief: this is not a spectrometer, the aim is for ultimate faint reach. If we have sufficient spectral resolution R to get a channel spectrum for fringe tracking, that is enough. As the wedge angle is an entirely free parameter with few other impacts, this is easy to optimize separately.

We take CL2 to be 350mm, and we wish for 6 pixels across the whole H band which corresponds to R of about 34 in H and this can easily be obtained by using a sapphire prism. The focal length of CL2 is longer than is ideal for this spectral resolution. Fortunately, the cross correlation of an Airy disk and a top hat function is quite forgiving so the reduction in spectral resolution is about two thirds of what one would expect by considering the size of the Airy spot alone. The choice of 350 mm for the focal length of CL2 will result in a group delay tracking range in H band of ±37 μm in H band and ±52 μm in K′ band.

Such a prism will deviate the beam overall by 9 degrees or so in H so the optical path will need a mild "kink" near the sensor. Alternative forms of zero-deviation dispersing prism should work fine if a kink in the vertical plane proves annoying. The simplest is a cemented pair of wedges of different Abbe number – straightforward to design and custom and not too difficult to procure.

Another option for the dispersive element is a modified retroreflector prism as show in Figure 4.

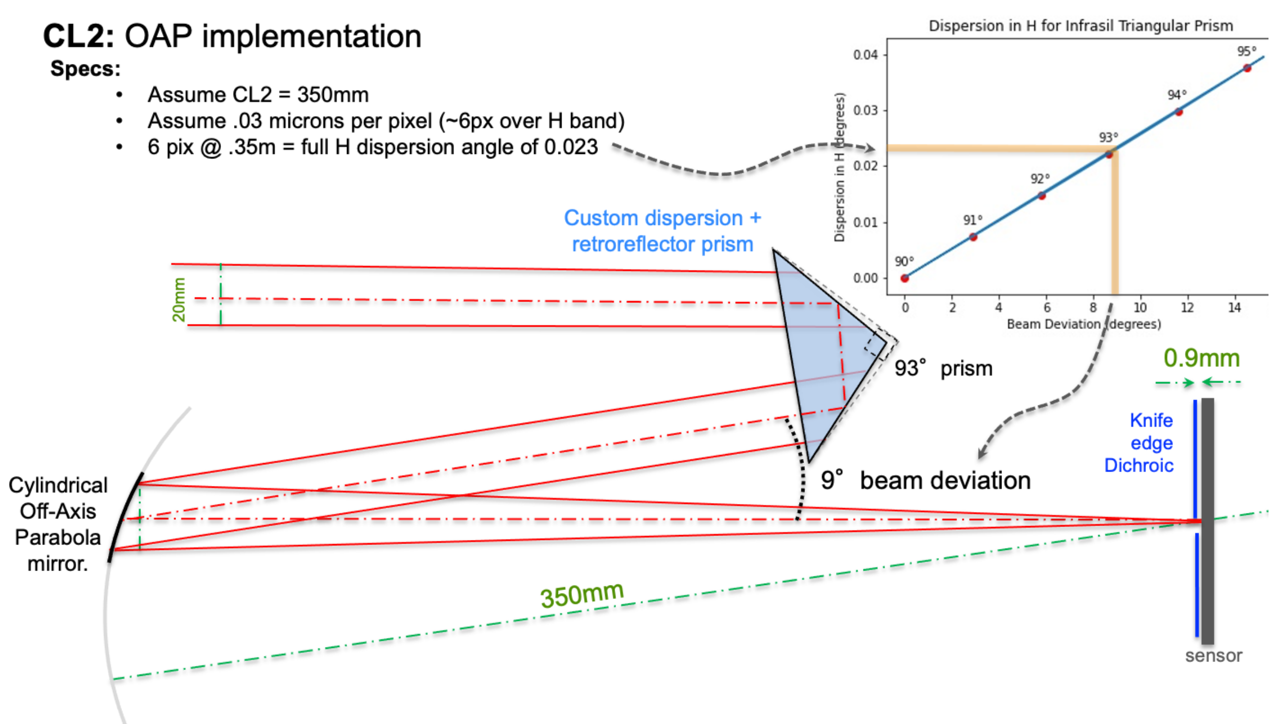

Figure 4. Using a modified retroreflector for a dispersive element. This has the advantage of keeping the number of optical elements low but is a specialize optic that would require a custom build. Note that the dimensions in this diagram are nominal and based on estimates made at the time it was drawn.

1.0 BACKGROUND COUNTS AND MODIFICATIONS TO THE FIRST LIGHT DEWAR

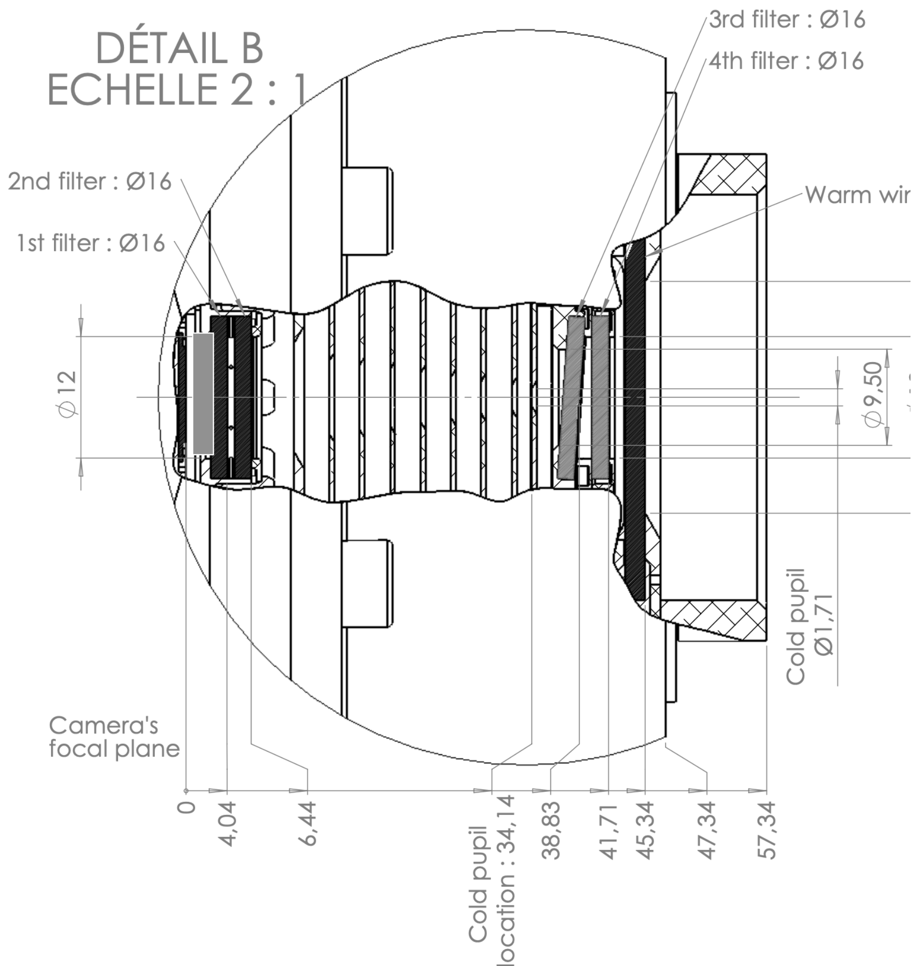

Figure 5. Layout of the input to the CRED-1 Camera. These dimensions are accurate and come directly from First Light.

The standard layout for the First Light CRED-1 dewar, as shown in Figure 5, comes with an F-20 circularly symmetric cold stop with a diameter of 1.71 mm and is specified to have a background count of 1100-1500 e/p/S when looking at a warm room. They also state that the background counts will be much the same with a warm mirror in front of the window as it is looking at the room. As a comparison in his document on background noise dated 2021/04/20, Mike Ireland estimated 1440 e/p/S for this arrangement. For a 10 mS exposure 1100-1500 e/p/S is the equivalent of 3.3-3.8 counts of noise.

There is room for four filters in this configuration, each 16mm in diameter and 1.6mm thick. The standard H&K configuration has a K (cutoff 2.45 μm) and H (cutoff 1.75 μm) filter in positions 1 and 2 and a second set of K and H filters in positions 3 and 4. We plan instead to use K′ (K-short) with a cutoff at 2.31 μm in order to reduce background and to match the filter currently in use in the existing camera NIRO, but in these calculations we conservatively assume the background of 1500 e/p/S for the 1.71mm diameter circular aperture of the standard F-20 system. We will also assume that the background counts scale with the square of the F ratio of the system, or equivalently, with the area of the first cold stop inside the camera.

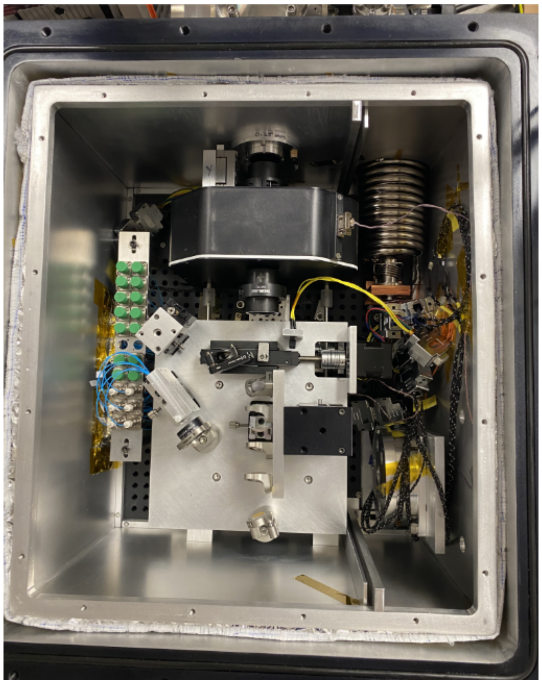

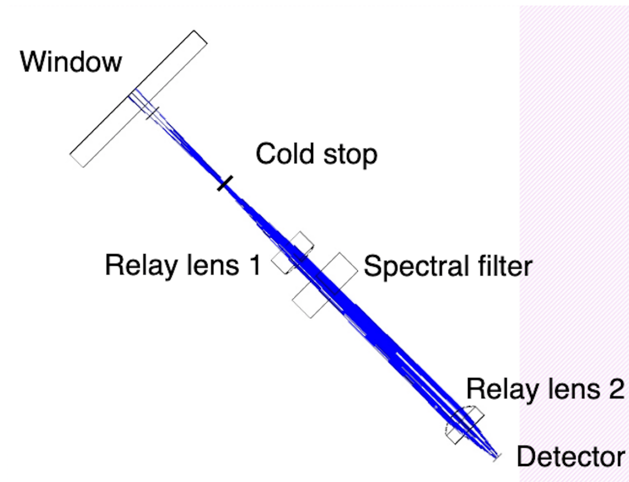

Figure 6. *Left:* The second dewar for MYSTIC. *Right:* Optical layout inside NIRO.

As a comparison, the MYSTIC CRED-1 camera, which is an F-4 system, has 35000 e/p/S background looking into a warm room. This makes sense as $(20/4)^2 \times 1500 = 37500$. Once the second dewar was added to the MYSTIC system there was a background of 350 e/P/S, an improvement of a factor of 100. For a 10mS exposure, this is the equivalent of 1.9 noise. The NIRO system used in the CLASSIC/CLIMB beam combiner has a background of 20000 e/P/S, the equivalent of 14.1 in noise over 10mS. Even without a second dewar if we use the F-20 system we have an improvement of a factor of about 4 over NIRO but are worse by a factor of 2 than the current MYSTIC setup with the second dewar.

We do, of course, plan to add a second dewar to the system in the second phase of development of this system, while in the first phase we will use only the dewar included in the CRED-1 camera. Our approach to adding the second dewar would be to copy, as much as possible, the MYSTIC design shown on the left of Figure 6, especially in terms of coupling the dewar to the camera. In this design the input window (top) for the camera is inside the second dewar. We would need to add an input window, a cold stop, and a single reimaging lens of the appropriate focal length. This would be very like the current NIRO design shown on the right of Figure 6 and is also very similar to the optical design in the original proposal.

The MYSTIC layout brought the background down by a factor of 100, while the NIRO layout has a factor of 10. Conservatively, if we get this factor of 10 improvement with the second dewar we will then be at the equivalent of 1.22 in background noise with the standard F-20 circular cold stop, which is an order of magnitude better than NIRO. This, combined with the sensitivity advantages of the image plane design over the aperture plane design of CLASSIC/CLIMB as well as the significantly lower readout noise, will have better sensitivity than the scheme laid out in the original proposal and will do significantly better than CLASSIC/CLIMB even without the second dewar.

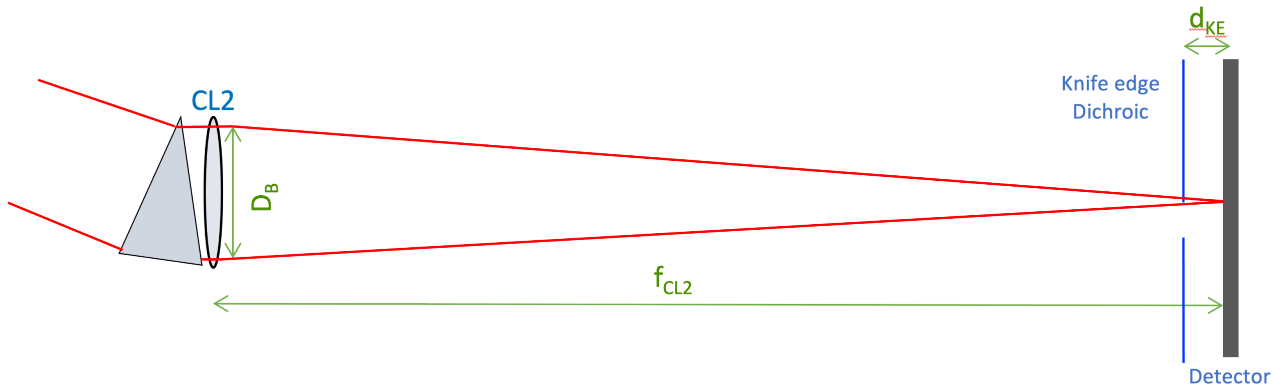

Figure 7. Geometry showing contamination of H band by K′ band light.

There is one primary area of concern, and that is contamination in the H band from background counts in the K′ band. This can be resolved by replacing the first filter in the camera as shown on the left of Figure 5 with a custom “edge filter” that has an H band coating only on the lower half. There are two problems with an edge filter such as this, both to do with how much K′ band light reaches the H band part of the detector.

The first issue is that some of the background light will diffract on the edge of the filter and reach the longest wavelength channel of the H band system. The Fresnel scale for diffraction is given by

$$d_F = \sqrt{\frac{x\,\lambda}{\pi}}$$

Where x is the distance from the refracting edge and the first filter in the camera is 2.4 mm away from the detector. For K′ band we will have a Fresnel scale of 40 µm. For the 24 µm pixel size and a gap of 6 pixels on the chip between H and K′ we have 3.2 Fresnel scale units, resulting in much less than 1% of the K′ band background light diffracting into the longest wavelength channel of the H band system and much less in the other pixels.

A more serious concern is the geometric contamination of light from K′ band in the converging beam as shown in Figure 7. The K′ band light will no longer reach the chip after a distance of

$$\frac{d_{KE}}{f_{CL2}} \times D_B$$

For the focal length of 350mm and the filter to detector distance $d_{KE} = 2.4$ mm this will be 130 µm or about 5.5 pixels while the gap between H and K′ bands is 5 pixels. This could be improved by either increasing the focal length of the CL2 optic, thereby reducing the spectral resolution of the system, or placing the filter surface much closer to the detector surface.

In Figure 7 we show a filter substrate design that will allow us to get to within 0.9 mm of the chip. This design was provided to us by First Light and according to them adds little risk compared to their standard filter design. A design like this would reduce the area of contamination to 2.5 pixels. However,

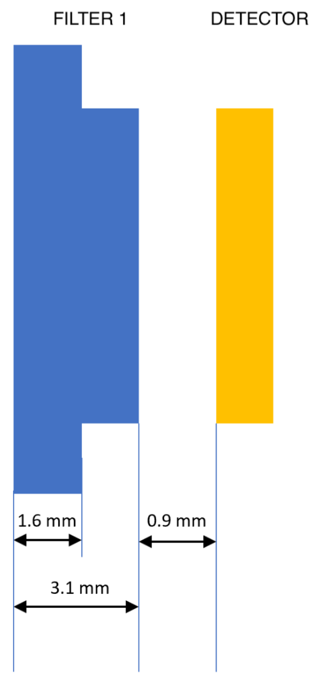

Figure 7. Proposed shape of edge filter to replace filter #1.

they made it clear that if we did provide this filter the risk would be ours and not theirs, so we think their protestations about low risk are to be taken with a grain of salt. Furthermore, this calculation assumes a perfectly sharp edge on the filter which turns out to be very difficult to make.

After numerous discussions with optical vendors, we have found that this custom shape filter and sharp edge boundary (specified as <50 μm) is very difficult to acquire. We contacted 10 companies who we have either used before or have been recommended by First Light or other members of the consortium. Most put in a no-bid, while the two that did bid gave prices of $18k and $50k. A third vendor has told us that they cannot make the odd shape we are asking for, as it will not fit inside their coating chamber, but can make a filter of the standard shape for the camera with a transition zone of the filter edge as small as 100 μm for a price of $5k. The amount of K′ light getting through now becomes an integral of the edge shape, assumed to be linear, and the beam shape, in this dimension rectangular, and we show in Figure 8 the final transition shape for a 100 μm edge boundary at various distances from the detector. At the default distance of 2.4mm we have less than 10% contamination of background light in the longest wavelength channel of the H band. We conclude that using the standard design, rather than a higher risk specialized shape, and a specification of 100 μm on the boundary edge will be fine for our needs.

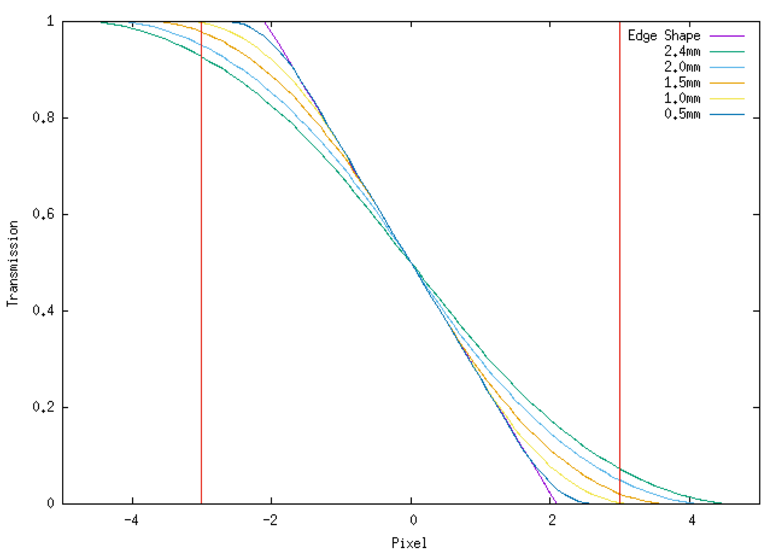

Figure 8. Effect of changing the distance between the edge filter and the detector chip for a 100μm 'edge' width. Red lines show the area between the H and K′ bands.

The final consideration is the shape of the cold input pupil. The beams are anamorphic so rather than use the default F-20 circularly symmetric cold stop, we plan to use a rectangular or square shape. First Light have done a preliminary design of a rectangular cold stop shown in Figure 9.

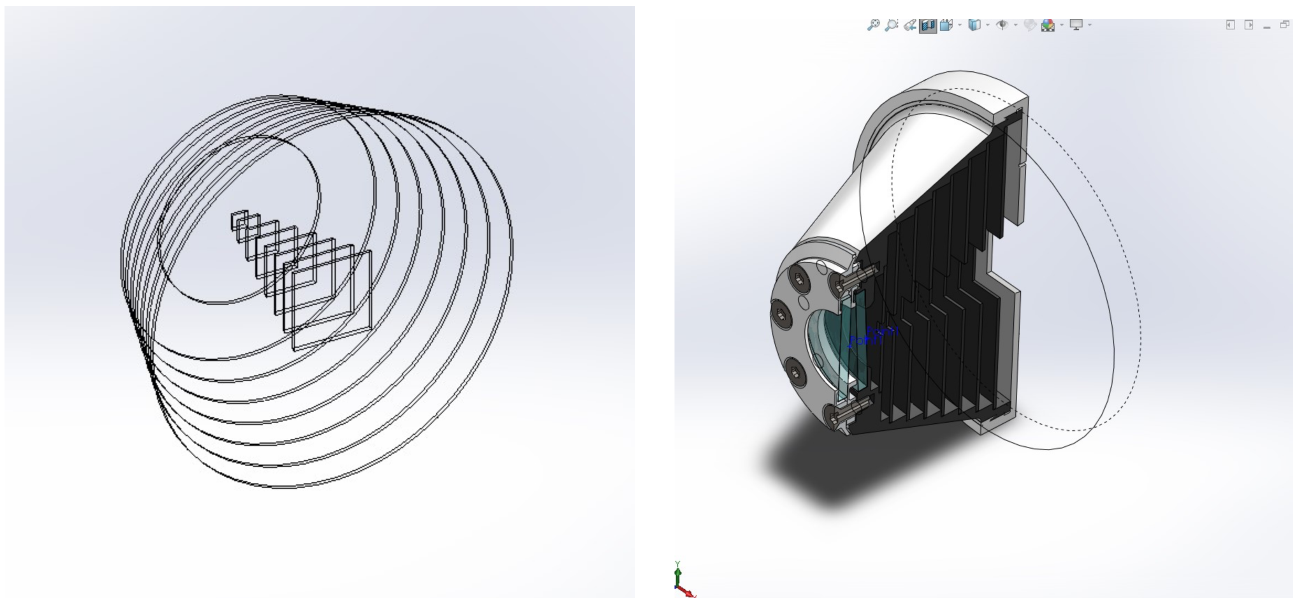

Figure 9. Proposed layout for a rectangular cold stop by First Light.

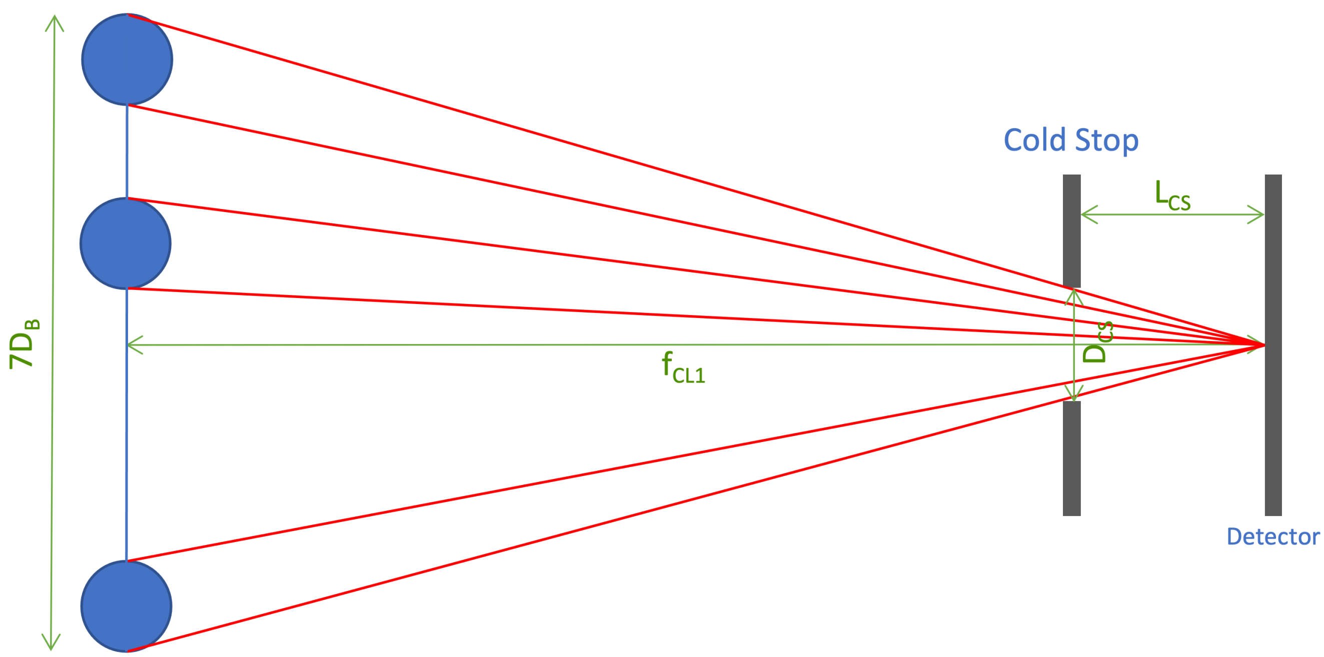

Figure 10. The geometry of the cold stop in the horizontal fringe axis.

The final dimensions of this rectangular cold stop are up to us to specify, and we show in Figure 10 the geometry of the horizontal fringe axis. Here we have a full width of $7D_B$with a common focus at a distance of f_{CL1}, while the cold stop is a distance L_{CS} away from the detector surface. Naively, the size of the cold stop in this axis would need to have a width of at least $\frac{L_{CS}}{f_{CL1}} \times 7D_B = 0.858$ mm. However, since the focal length of CL1 is so large, we are in the far field here and we must consider the size of the Airy disk at the longest wavelength. The width of the cold stop is therefore given by

$$CS_{Width} = \frac{L_{CS}}{f_{CL1}} \times 7D_B + \frac{2.44\,\lambda}{D_B} \times F_{CL1} = 2.44 \text{ mm}.$$

A diagram for the geometry that determines the vertical size of the cold stop is given in Figure 11.

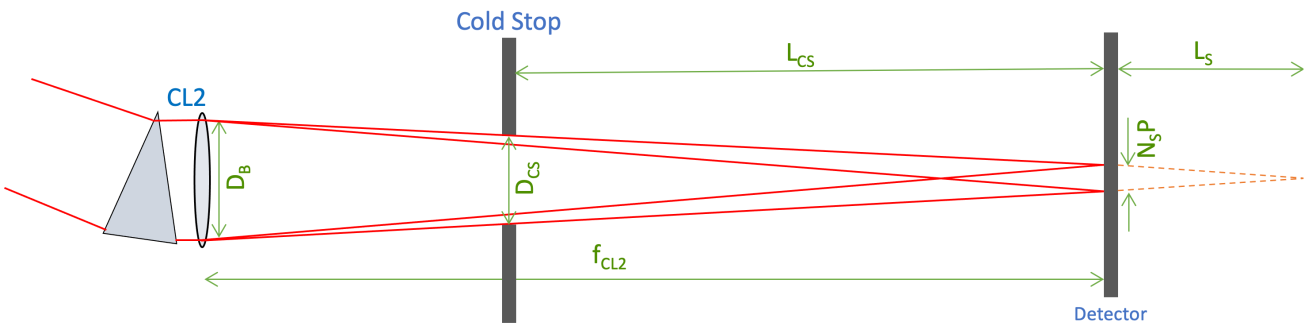

Figure 11. The geometry of the cold stop in the vertical spectral axis.

In this case we have a pseudo focal point behind the detector of

$$L_S = \frac{N_S\,P\,f_{CL2}}{D_B - N_S P} = 10.9 \text{ mm},$$

where N_S is the number of pixel in the spectrum, which we set at 24 to include the extra pixels needed to include the size of the Airy disk in the spectral direction. We can then calculate the required size of the cold stop to be

$$CS_{Height} = \frac{D_B\,(L_S + L_{CS})}{f_{CL2} + L_S} = 2.34 \text{ mm}.$$

We therefore will specify a square cold stop off dimensions 2.5 $\times$ 2.5 mm with an area of 6.25 mm^2. This is a factor of 2.72 larger in area than the standard circular F-20 cold stop and should produce 4082 e/P/S of background in the K′ band, a factor of 5 less than the current NIRO system which could then be further reduced by at least another order of magnitude by the second dewar. From a background and readout noise perspective this will gives us 1.1 magnitudes of sensitivity over CLASSIC/CLIMB and this estimate does not include the other advantages of the image plane combination scheme as shown in TR103 which could be as much as another 2 magnitudes. This increases to 3-5 magnitudes if the second dewar performs as well as the one built for MYSTIC. All of this is based on very conservative assumptions, and we are hoping to do significantly better. The sensitivity will be much greater in H band as there will be little or no background. We conclude that this design more than meets the criteria of the original proposal.

5.0 PHOTOMETRIC CHANNELS

We have so far ignored the issue of photometric channels on the basis that we are not including spatial filtering in this design, but it should be possible to add them to the design of the second dewar.

6.0 MULTIPLEXING FOR 6 BEAMS: 2x3 BEAM COMBINERS

It turns out, partly by lucky coincidence of the beam geometries required and the sizes of components such as the detector and location of the cold stops, that a second triad of 3 beams can be identically imaged onto the sensor with no impact at all on the performance of the first set of 3. This is accomplished by nominating a single common cold-pupil at some intermediate plane where the two sets of beams exactly cross over. This common cold-stop is denoted CS3 in the drawings of Figure 12, and is ideally situated about 60mm in front of the sensor. Note that this location is convenient: just forward of the camera housing in a second-phase project stage where there is a cold fore-optics chamber available. The second set of 3 beams will also comfortably pass the internal camera cold stop and so can also be implemented at an earlier project stage. Note that this optical scissors or "crossover" design between the left-3 and right-3 beam sets means no enlargement or change to the critical cold stops in

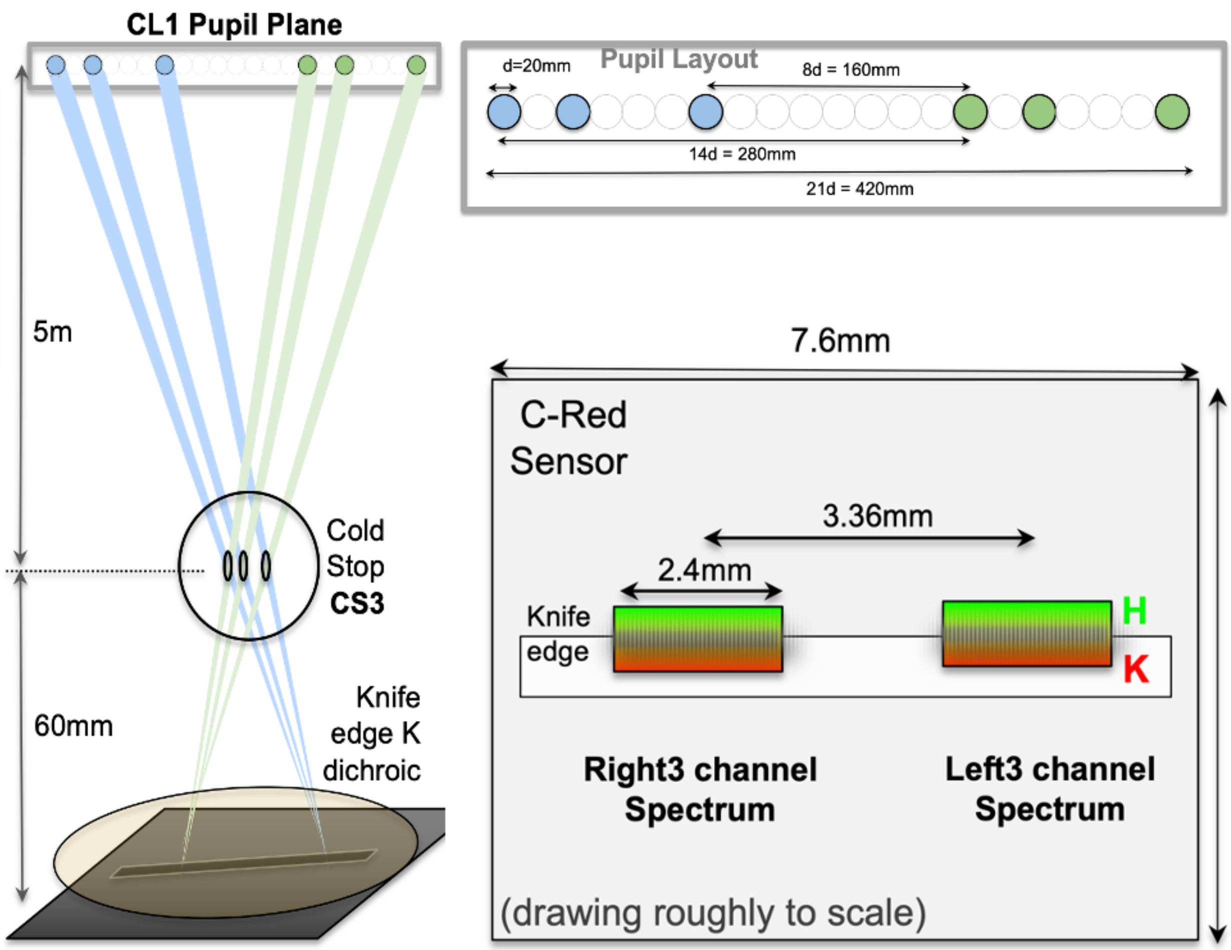

Figure 11. *Left:* Beam layout for 2x3 way beam combination. *Above Right:* Geometry of beam layout. *Below Left:* Position of fringes on detector. Note that the dimensions in this diagram are nominal and based on estimates made at the time it was drawn.

this region, so that they may be optimized, and the second set of beams added with no compromise.

The fortuitous part of the design is that the entire optical setup just works neatly and naturally from that point onwards. The twin pair of interferograms are displaced on the sensor by about 3.4mm. This is sufficient to prevent any significant cross talk between the left- and right- set of 3, and also comfortably spans the available real-estate on the sensor without encroaching on the edges (see Figure 12). Furthermore, the other key elements – the horizontal knife-edge and the vertically-oriented dispersing element – all work identically for both pairs of 3 beams. Two sets of three can be accommodated just as comfortably as a single set of three, and with no design compromise required.

A final, perhaps speculative comment on this configuration. The pupil layout for 2x3 beams places a gap between the left-3 and right-3 ideally 8 times the unit beam diameter (see Figure 12). For a moment if we forget 2x3 beams and think about a single 1x4 beam combiner, we can see from the figure that the non-redundant spacings are, by dumb luck, exactly appropriate for this. There are two possible examples: the left-3 (blue) plus one of the right (green), or the other way around. Of course, the speculative nature of this throw-away comment is noted: Nyquist sampling a 1x4 beam combiner would require a doubling of the focal length onto the sensor. A future downstream image-magnifier mode would be needed, but the awkward upstream cylindrical mirrors work just as they are.

7.0 CONCLUSION

We are confident that the design outlined here with CL1 having a focal length of 5.371m and CL2 of 0.35m is workable and will allow us to send the beams directly into the camera as well as to further augment the efficiency of the cold stop using a second dewar in the future. The design is simple and has a minimum number of optical components, producing the pattern we need directly on the detector with, or without, a second dewar. The high-risk items are: (1) the long focal length cylindrical lenses and (2) a knife-edge H band filter inside the CRED-1 dewar. We continue to pursue these items and have placed the order for the CRED-1 camera.

We plan the following development path:

1. Assemble the input optics and test the system using the STS (internal light source) and the engineering H band camera. This camera works in H band only and has a pixel size of 15 μm. Many of these tests could be done with a single beam and optical chain just to measure image quality. This won't be useful on the sky but can be done in the short term with low risk.
2. Replace the engineering camera with the CRED-1 camera. This will still be dominated by background, but not so much that we cannot test it on the sky. This will have less background in K′ than NIRO, as well as low background in H and the sensitivity benefits of an image plane combiner as described in TR103. There would be useful science to be done and we will get a good feel for how bad the background really is, if the edge filter works as expected, and what we can expect once we add the second dewar and a cold stop. An additional inexpensive strategy that might be tested in this stage is the use of a Narcissus mirror to stand in for the future cold stop CS3. Although they should work in theory, real-world reports of the utility of Narcissus mirrors seem mixed. On the other hand, they require low optical quality and should be inexpensive to trial.
3. In parallel start design work on the second dewar. The lead time for this can be longer and we should have learned much from steps 1 and 2 to fold into the design. For example, if the edge filter does not work as expected we could implement a Heimdallr like design in the second dewar to separate H and K′ bands. We will also have a better idea concerning the need for photometric channels.

APPENDIX A

We have a built a small spreadsheet that includes all of these, and other calculations to allow us to investigate the consequences of changing any of these parameters.

SILMARIL OPTICAL CALCULATIONS
12/16/21

Black Numbers are inputs. Blue numbers are calculations.

Beam Diameter (m) 0.01905

Spectral Bands are based on current NIRO filters

Band	Lambda0	dLambda	Lambda Low	Lambda High
H	1.6350E-06	2.9000E-07	1.4900E-06	1.7800E-06
Gap	1.8850E-06	2.1000E-07	1.7800E-06	1.9900E-06
K	2.1500E-06	3.2000E-07	1.9900E-06	2.3100E-06

CRED-ONE Camera specification from First Light

CRED-1 Cold Stop/Baffle	Filter 4-Detector (m)	LCS = CS to Detector (m)	CS Diameter	CS Area (mm^2)
	0.0024	0.03414	0.00171	2.30
	Pixel Size	**Cold Stop F Ratio**	**BG e/P/S**	**Read Noise**
CRED-1 Camera	2.4E-05	20.0	1500.0	1.00

Other Cameras

	BG e/P/S	Cold Stop BG Reduction	BG with CS e/P/S	Read Noise
MYSTIC with F4	37368.5	100.0	374	1.00
NIRO	20000	10.0	2000	9.80

We assume we will get the geometric mean of these when we add a second dewar

CRED-1 Camera		31.6		1.0

HORIZONTAL Axis - Interferometry

	Maximum Spacing (D)	Min Pix/Frg	#Fringes/Airy Disk	
Fringe Axis	7	2.5	17	
	H Band Minimum	**H Band Maximum**	**K Band Minimum**	**K Band Maximum**
#Pixels across Fringes	43	51	57	67

We can now set the focal length of the first cylindrical Lens

CL1	Combined Focal Length	F Ratio	Radius of Curvature	Required DM Stroke (u
Single Beam	5.408	283.86	10.82	4.19
	Beam Diameter (m)	**F Ratio**	**Airy Disk Size (mm)**	
All three beams	0.13335	40.55	1.60	

VERTICAL Axis - Spectral Resolution

	#Pix H Band	Width (m) in H Band	Spec Resolution	#Pix Gap	#Pix K Band
Spectrograph	6	4.83E-08	33.8	5	7
Total #Pix	18				
Number of Pixels Read	990				

We can now set the focal length of the second cylindrical lense

	Focal Length (m)	F Ratio	Airy Disk Size (um)	LS (Behind Det) m
CL2	0.35	18.37	103.56	0.0100

This sets the Airy disk size in the vertical axis

	H Band	Gap	K Band
Airy Disk Size (m)	7.3296E-05	8.4503E-05	9.6383E-05
Airy Disk Size (Pix)	3.05	3.52	4.02

This sets the spectral resolution

Smearing Ratio	1.48	1.65	1.84
Smearing Width (m)	7.17E-08	7.95E-08	8.90E-08

This results in a Group Delay Tracking Range

GDT Range (um)	37.3	44.7	51.9

Cold Stop Dimmensions

	Horizontal Size (mm)	Vertical Size (mm)	Area (mm)	Ratio with Detector
Cold Stop Size	2.44	2.34	5.70	0.84
Round Up	2.50	2.50	6.25	0.80
Over sizing (mm)	0.06	0.16	0.11	**Ratio with F20 CS**
Adjustability	0.032	0.091	0.062	2.72
For Square Vs Round at F20	2.50	2.50	6.25	1.27

This will determine the amount of background counts

Square CS at Same Position	BG e/P/S	Sigma BG (10mS)	Sigma (BG+RN)	Improvement	Magnitude
NIRO	20000	14.1	17.2	1.0	0.00
No second Dewar	4082.2	6.4	6.5	2.7	1.06
NIRO type improvement	408.2	2.0	2.3	7.6	2.21
Geometric Mean	129.1	1.1	1.5	11.4	2.64
MYSTIC type Improvement	40.8	0.6	1.2	14.5	2.90

Image Vs Aperture Plane	#Pixels For Image Plane	#Pixels For Aperture Plane	Sample Time Ratio	Improvement	
	67	68	5	2.3	0.89

#Airy Disks	Airy Disk Size	Separation of 1-3/4-6	Total Width
2	1.5999E-03	0.504	0.637

Edge Filter

	Fresnel Scale (m)	Fresnel Scale (Pix)	Fresnel Scale/Gap
Diffraction On Edge	3.37E-05	1.41	0.28

	Size of Shadow (m)	Size of Shadow (Pix)	Shadow/Gap
Shade on Edge	1.31E-04	5.44	1.09

	Size (m)	Size (Pix)	Trans/Gap
Filter Transition Zone	1.00E-04	4.17	0.83